International Journal of Fracture **95:** 221–238, 1999.

Scaling phenomena due to fractal contact in concrete and rock fractures

M. BORRI-BRUNETTO, A. CARPINTERI and B. CHIAIA
Department of Structural and Geotechnical Engineering, Politecnico di Torino, 10129 Torino, Italy
e-mail: chiaia@polito.it

Received 10 July 1998; accepted in revised form 18 December 1998

Abstract. Concrete-to-concrete friction contributes in many cases to the stability of a structure. At different scales, the slope stability of rock joints is deeply influenced by the surface morphology and shows a marked size-dependence. In this paper, the closure and sliding-dilatant behaviour of cracks in concrete and rocks is investigated by means of a coupled numerical/experimental approach. These natural interfaces show self-affine properties in the relevant scale range. Attention has been focused on the stress transfer mechanism across the interfaces, showing that the sets of contact points possess the self-similar character of lacunar fractal sets. Scaling laws come into play and the size-effects on the shear strength of rough interfaces, and on their closure deformability, can be explained.

Key words: Size-effects, fractal geometry, fracture interface strength, contact mechanics.

1. Introduction: frictional behaviour of cracks in concrete and rocks

Concrete-to-concrete friction comes into play in many situations and contributes to the stability of a structure. However, the effects of friction are especially valuable in massive structures, because the frictional contribution to stability is size-dependent, if dead loads are considered. Within the classical hypotheses (Johnson, 1985) the frictional force T is independent of the nominal contact area A_n, but depends on the true contact area A_r, which, in turn, is proportional to the normal load $F (T = \mu F)$. If perfectly similar structures are considered, the nominal contact area scales according to L^2, whereas the dead loads (and the frictional force) scale proportionally to the weight of the structure, that is, according to L^3. Therefore, if $\tau = T/A_n$ is the frictional specific resistance, one obtains $\tau = T/A_n \sim L^3/L^2 \sim L$. Hence, stability due to friction increases with the size scale of the structure. Note, however, that this is no longer true when the shear actions also depend on gravity (e.g. seismic loading). The evaluation of the interface shear transfer capacity T_u is based on the traditional theory of friction, that is, T_u is proportional to the normal load F by means of a friction coefficient μ. The value $\mu = 1.4$ is suggested by Park and Paulay (1975) for concrete cast monolithically, while $\mu = 1.0$ applies for concrete placed against hardened concrete.

In concrete dams, because of the joints generated by a stepwise construction of layered concrete blocks, and because of the strong thermal gradients, large cracks can be present from the beginning of their life. The assessment of safety under the presence of the cracks cannot be adequately addressed if the shear resistance of these joints is not taken into account. In many concrete structures, shear forces may cause a sliding type of failure along a pre-existing plane. Because of external tension, shrinkage, or other causes, a crack may form along such plane even before shear occurs. Thus, the possibility of shear transfer by friction arises.

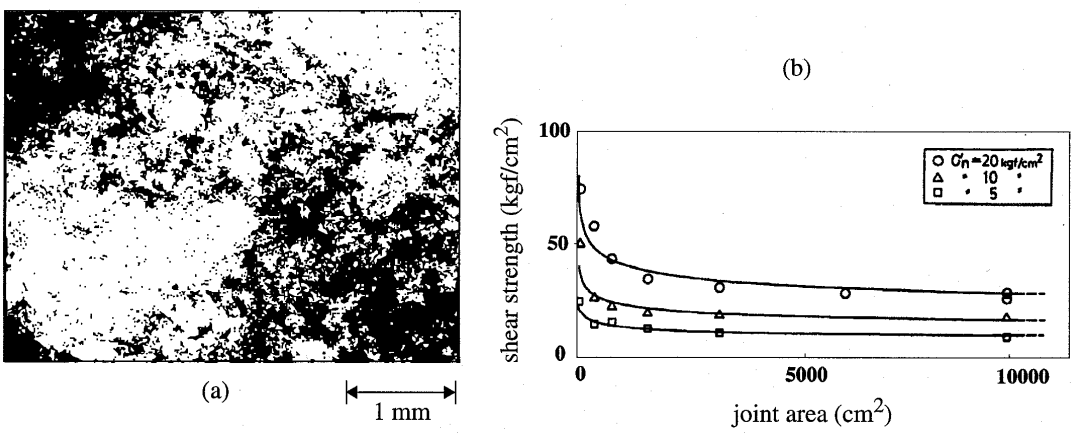

Figure 1. (a) Experimental contact domain in a natural rock joint at a mean apparent stress of 85 MPa (Cook, 1992). (b) Experimental decrease of the measured shear strength for increasing specimen size (Yoshinaka et al., 1993).

Earthquakes showed that construction joints in some members, particularly shear walls, form the weakest link in the load-resisting mechanism of the structure if large shear forces need to be transmitted.

Frictional effects in cracked flexural members can be critical only if the span to depth ratio is very small (deep beams). In these members, concrete friction is often accompanied by the dowel action of the longitudinal bars subjected to shear displacement. In fact, even a small shear displacement v is accompanied by a normal displacement δ of the crack faces (*dilatancy*). To develop an acceptable friction capacity, dilatancy must be limited by normal loading, provided by external constraints or by the steel bars. Dilatancy may also reduce the durability of a joint, for example in seismic areas. If the bars reduce dilatancy, the interface shear transfer capacity increases. Thus, less shear displacement occurs and less deterioration of the shear capacity can be expected after a few cycles of high-intensity loading. Instead, if cracks are free to open, repeated loading will cause a deterioration of the interface roughness, with a corresponding reduction in the shear capacity.

At scales different from the usual scales of concrete structures, the engineering analysis of rock structures, like slopes, excavations or tunnels, needs a model of the mechanical response of the rock mass. Far from being a continuum, the rock mass is a complex system composed of blocks and fractures. In many cases, a detailed study of the morphology and of the behaviour of discontinuities subjected to normal and shear forces is necessary to evaluate, say, the factor of safety of a slope or a foundation. In this respect, it is worth mentioning the review paper by Cook (1992), where most of the basic mechanical issues are reported. In that paper, the crucial importance of the effective stress transfer at the interface is addressed (Figure 1a).

The measurement of the shear strength of natural discontinuities is usually obtained by means of laboratory testing on rock joints. The influence of the roughness of the contacting surfaces, as well as the importance of scaling in the assessment of the *in situ* resistance, is a well-known fact (Pinto da Cunha, 1993). Experimental tests showed a marked size-dependence of the shear strength of rock discontinuities (Figure 1b). A number of constitutive phenomenological models have been proposed with the purpose of estimating the most plausible full-scale strength parameters starting from data obtained on small scale specimens. The classical empirical approach of Barton and Choubey (1977), based on visual estimation of

roughness of joint profiles, was extended in order to take into account the scale dependence of strength (Bandis et al., 1981), and is perhaps the most widely used shear strength criterion in rock engineering. Further attempts tried to get a more objective determination of the parameters through mathematical treatment of geometrical data obtained from surface analysis. A remarkable effort was due to Scholz and co-workers (Brown and Scholz, 1985; Yoshioka and Scholz, 1989; Wang and Scholz, 1993). In these works, the mechanical response of a rock interface is studied as a result of the interaction of asperities, paying attention to the real topography of the contacting surfaces.

2. Contact between rough surfaces: traditional models and fractal approach

A realistic characterization of the topography of rough surfaces represents a crucial point in the modelization of interface phenomena. Many tribologic phenomena, like friction, lubrication and wear of mechanical components, strongly depend on the surface morphology (Johnson, 1985). At the same time, the thermo-electric conductivity between two bodies in contact is intimately related to the interface characteristics.

The earliest attempts to extend the Hertzian theory of elastic contact between smooth bodies to real bodies with rough boundaries can be ascribed to Archard (1957) and to Greenwood and Williamson (1966). Archard was the first to solve the discrepancy between the classical Hertzian solution and the experimentally validated Amontons's law. This law is based on the hypothesis that the frictional force T is proportional to the area of true contact A_r , which, in turn, is proportional to the normal load F. While, in fact, Hertz had shown that, in the case of smooth spheres, the real contact area A_r is related to the normal load F by a nonlinear relation ($A_r \sim F^{2/3}$), Amontons's law stated the direct proportionality between frictional force and normal load ($T = \mu F$). By means of a hierarchical model of hertzian spheres with progressively decreasing radius, Archard obtained the overall linear behaviour ($A_r \sim F$) requested by the experimental evidence.

Greenwood and Williamson (1966) considered one of the bodies in contact to be rough, with contact occurring at a number of discrete points. The asperities could undergo only elastic deformation, and at the top of each peak an Hertzian micro-sphere was supposed to exist. The asperities were modelled in a way for the peaks to follow a Gaussian distribution around a mean flat surface. The area of true contact was determined to be approximately proportional to the load, so that the basic hypothesis of the theory of friction could be supported also for purely elastic contact. The authors concluded that the behaviour of rough surfaces is determined primarily by the statistical distribution of asperity heights and secondarily by their mode of deformation. Thus, although plastic deformations cannot be excluded, at least for the highest and sharpest peaks, it was argued that no new features would be introduced by plasticity.

Because the interface phenomena involve all length scales, a scale-independent description of the surfaces should be pursued. Nevertheless, classical models as the one by Greenwood and Williamson (1966) make use of statistical parameters, like the mean and variance of the surface elevations, of the slopes and of the curvatures. Unfortunately, all these quantities, whose experimental determination is questionable, are strongly dependent on the resolution adopted for the description of the interface (Majumdar and Bhushan, 1990). On the other hand, the theory of fractals sheds new light on the Archard's model, which is, indeed, scale-independent. Archard's model can be thought of, in fact, as the first deterministic (pre-)fractal model applied to contact problems, as already pointed out by Ling (1989).

Recently, random fractal models of rough surfaces (Mandelbrot, 1982) have been shown to resemble very closely the morphology of natural and man-made surfaces. The surfaces of magnetic tapes and of metallic components, as well as natural boundaries like fractures and rock joints, show fractal properties over a wide scale range. This implies the morphological invariance (in the statistical sense) of the surfaces under a group of affine (anisotropic) scale transformations. Self-similarity is a particular case of the more general concept of *self-affinity*. Self-similarity, in fact, is characterized by isotropic dilatation symmetry and by the absence of an internal length scale. The scaling relation of a self-affine surface $z(x, y)$, if r is the scaling (or magnification) factor, can be written as:

$$f(x, y, z) \rightarrow f(rx, ry, r^H z), \tag{1}$$

where $H < 1$ is called the *Hurst exponent*. Equation (1) implies that the vertical coordinates scale less than the horizontal ones. Thereby, sharper details appear in the surface as finer resolutions are adopted. The fractal dimension is obtained as $\Delta_{\mathcal{G}} = 3 - H$, and thus these 'surfaces' are invasive fractals ($\Delta_{\mathcal{G}} > 2.0$). According to the experimental evidence (Carpinteri, 1994) and to the theory of dissipative phenomena, the fractal dimension of a Brownian surface ($\Delta_{\mathcal{G}} = 2.5$) often represents the upper limit of disorder. This is the case, for example, of fracture surfaces. Therefore, for most natural surfaces, $0.5 \leqslant H \leqslant 1.0$.

Panagiotopoulos and Panagouli (1997) adopted an engineering-oriented fractal methodology to solve problems of unilateral and adhesive contact and problems of friction. Their numerical procedure exploited the approximation of fractal boundaries through classical surfaces of integer Hausdorff dimension (Iterated Function Systems). Borodich and Mosolov (1992) modelled polished fractal surfaces by means of Cantor punches. The problem of indentation was solved for this geometry, in the case of elastic as well as of plastic bodies. Using asymptotic methods, they obtained power-laws for the dependence of the load on the depth of the indentation. The exponents of the power-laws depended explicitly on the fractal dimension of the punching set. Warren and Krajcinovic (1995) developed a Cantorian fractal model, similar to the one by Borodich and Mosolov, and extended the discrete model to a continuous formulation of the elastic-perfectly plastic deformation model.

Regarding recent experimental investigations, it is worth mentioning Majumdar and Bhushan (1990), who adopted an optical profilometer to digitize magnetic tape surfaces. They used the Weierstrass-Mandelbrot fractal function to model the surface roughness, obtaining good correlations with experimental data. Majumdar and Tien (1990) carried out tests on various machined steel surfaces and textured magnetic thin-film disks. The power-law spectral behaviour of these surfaces unequivocally proved that statistically similar images of the surfaces appear when the surface is repeatedly magnified. However, although the self-similarity of the contact domain is exploited in their model, the mechanical quantities retain their usual physical dimensions. On the contrary, finite measures of fractal domains can be obtained only by means of noninteger dimensions. Accordingly, the physical quantities defined over these sets have to assume noninteger (anomalous) dimensions.

3. Anomalous scaling in the contact mechanics of natural interfaces

From a kinematical point of view, the linear elastic normal contact between two rough surfaces can be reduced, under some assumptions, to the problem of the so-called *composite topography* (given by the *sum* of the heights of two corresponding points in the undeformed

condition) pushing against a flat plane. The mechanics is controlled by the following physical variables: the external normal force F ([F]), the elastic modulus E ([F][L]$^{-2}$), a linear representative size of the contact area b ([L]), the interface closure displacement w_{int} ([L]), and a morphological parameter of the interface, e.g. the standard deviation σ_z ([L]) of the heights of the composite topography. According to the well-known Buckingham Theorem, there are three independent nondimensional groups, which can be determined in a straightforward manner. A scale-independent complete description of the mechanics of normal elastic contact can be obtained by simply finding the mutual relations among $\Phi = F/Eb^2$ and two other nondimensional quantities, for example $\xi = \sigma_z/b$ and $\omega = w_{\text{int}}/b$. A scale-independent governing relation $\Phi = \Phi(\xi, \omega)$ could be found. However, experimental investigations (e.g. Sage et al., 1990) provide data which do not fit in the nondimensional framework. This means that anomalous scaling occurs in the phenomenon.

Suppose, in fact, we are interested in extrapolating the nondimensional full-scale crack closure law $\Phi(\omega)$ from the laboratory tests. According to the nondimensional description, one should expect that w scales proportionally to b, if a self-similar phenomenon were considered (i.e., if σ_z were perfectly proportional to b). Keeping the elastic modulus E constant, similarity would imply that, if $b \to 2b$ moving from the model to the prototype, then $F \to 4F$ and $\sigma_z \to 2\sigma_z$. In practical words, if the linear size of the full-scale structure is twice the linear size of the model, a double closure value $2w_{\text{int}}$, under the same nominal pressure $\sigma_n = F/b^2$, can be obtained only if the standard deviation σ_z of the heights of the model's interface is doubled. Instead, when testing specimens of different size, *obtained from the same joint*, it is impossible to realize the condition $\sigma_z \to 2\sigma_z$ as $b \to 2b$. Schmittbuhl et al. (1995) affirmed that the standard deviation of heights, in natural rock discontinuities, far from being scale-independent scales with b according to

$$\sigma_z \sim b^H, \tag{2}$$

where $H = 3 - \Delta_{\mathcal{G}}$ is the Hurst exponent of the self-affine composite topography. Statistical investigations yielded the value $H \approx 0.8$ for natural joints, whereas the value $H = 1$ (corresponding to $\Delta_{\mathcal{G}} = 2$, that is, to Euclidean surfaces) would be necessary to ensure perfect similitude.

4. Fractal analysis of real interfaces and numerical simulation of contact

In a previous paper by Borri-Brunetto et al. (1998), three mathematical self-affine surfaces were adopted for the contact simulation. In this paper, instead, real interfaces are considered, namely a rock joint and a concrete fracture surface. The rock joint has been obtained from a cylindrical specimen of fine-grained sandstone fractured at midspan in three-point bending. The diameter of the specimen was equal to 50 mm. The concrete fracture surface was obtained from a bone-shaped specimen broken under uniaxial tension.

The experimental acquisition technique, extensively described by Carpinteri et al. (1999), consists of a laser profilometer moving in the two orthogonal directions X and Y by means of two micrometric step-motors. At each point of a horizontal grid, with spacing equal to s, the laser reads the height of the corresponding surface point. Therefore, the digitized surfaces, as well as any computer-generated surface, are only images (*pre-fractals*, characterized by a precise value of the resolution s) of the fractal set, which is a limit concept for $s \to 0$.

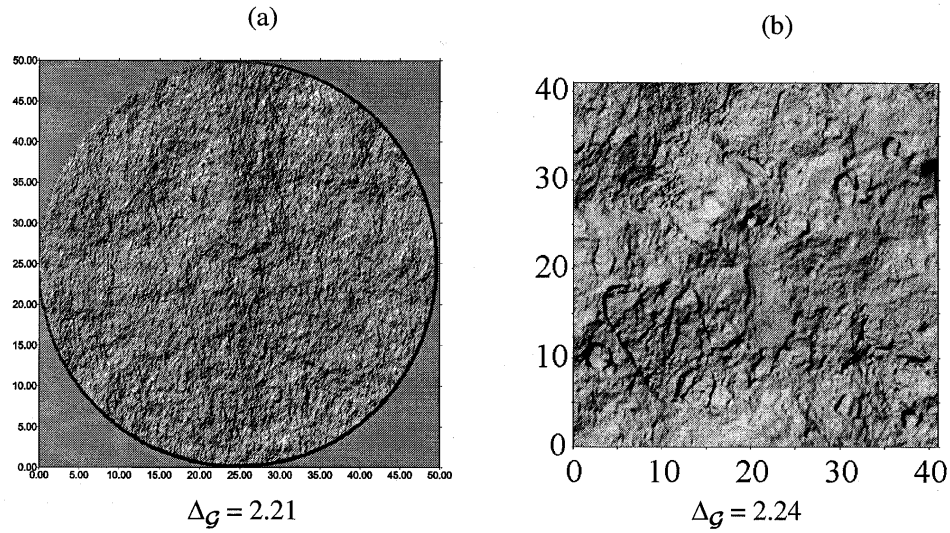

Figure 2. Shaded relief of the digitized fracture surfaces obtained from the sandstone specimen (a) and from the concrete one (b).

Shaded rendering of the rock and concrete surfaces are shown in Figures 2a and 2b, respectively. The scanned area measures $\pi(25)^2 = 1962\,\text{mm}^2$ in the case of the rock and $40 \times 40\,\text{mm}^2$ in the case of concrete. The digitisation interval s was set equal to 100μm and to 80μm, respectively for rock and concrete. It is believed that further refinements (a limit precision of 2μm can be attained by the laser) would not alter significantly the numerical simulation of contact, at least in the desired mesoscopic scale range. In both cases (concrete and rock), only one side of the fracture was digitized, because the hypothesis of initially perfectly matching surfaces at the opposite sides of the fracture is implicitly assumed in the following.

By applying both deterministic and statistic fractal tools the fractal dimension $\Delta_{\mathcal{G}}$ of the rock surface results to be comprised in the range 2.16–2.25, with a mean value equal to 2.21. The fractal dimension of the concrete surface can be set in the range 2.15–2.29, with a mean value equal to 2.24.

The concrete and rock joints are modelled by two linear-elastic half-spaces exchanging forces through the rough fractal surfaces described before. The unilateral contact problem has been extensively approached by many authors as a nonlinear optimization problem (e.g. Panagiotopoulos, 1985). In the present scheme, instead, an *active set* strategy has been preferred, to reduce the storage requirements for the computation. The model we have chosen leads to a simple solution, still retaining some of the most important features of the real phenomenon.

The numerical procedure is designed in order to determine the geometrical properties of the contact domain $\mathcal{D}$ between the half-spaces. In particular, we focused on the consequences of varying the *resolution* in the representation of the interfaces undergoing contact. With the attempt to study the behaviour of the interface taking into account the shear displacement, different normal contact simulations have been carried out by shifting one side of the joint, with respect to the other, by a certain offset v. A discrete version of the problem is considered, by introducing in the reference plane $X - Y$ a square grid of points with spacing s. Of course, s can be referred to as the resolution adopted in solving the problem and, in this

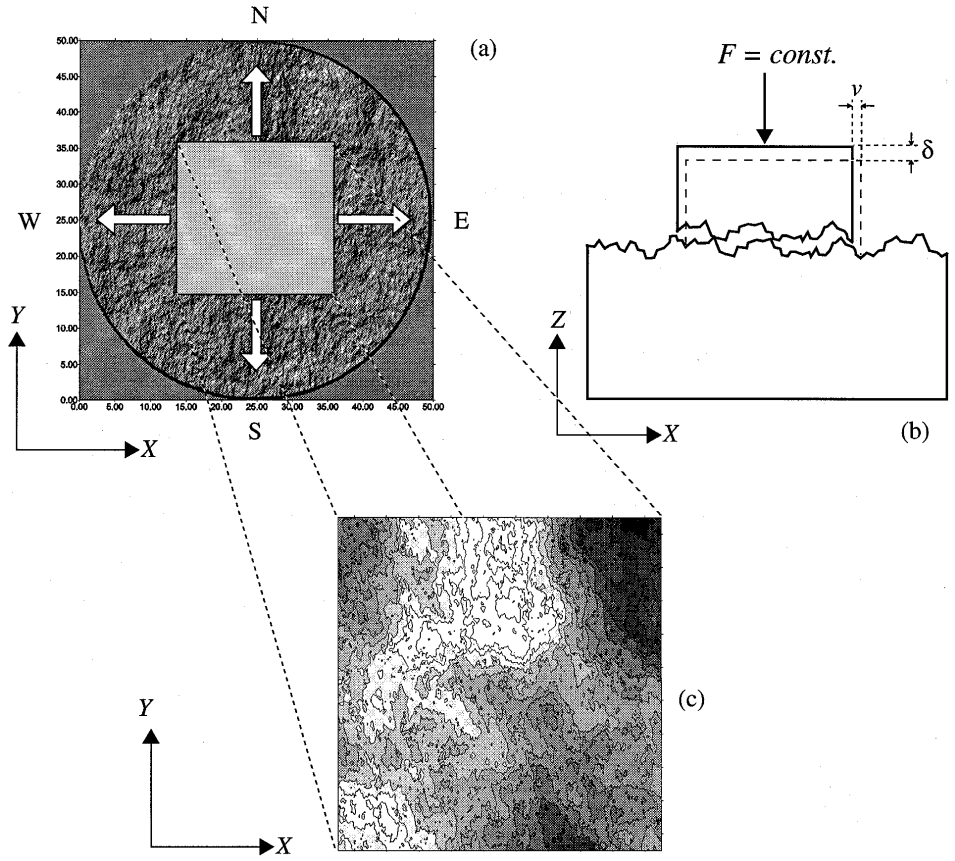

Figure 3. Scheme of the numerical simulation on the rock joint: dilatancy δ, shear displacement v, and composite topography (c) obtained for $v = 10$ mm.

case, corresponds to the digitization resolution. At each node of the grid two facing points at the opposite sides of the crack can touch and transmit a force. We assume a small contact zone to be involved around the grid point, whose area is related to the grid spacing s.

Once the offset v (in the $X - Y$ plane) between the initially perfectly matching surfaces is fixed, a relative closure displacement w (in the Z direction) is imposed to the half-spaces (Figure 3). The solution is sought in terms of pressure and surface displacements, paying attention to the unilateral condition at the interface. The approximations introduced as a first approach to the problem are:

(1) surface points displacements are perpendicular (Z direction) to the boundary mean plane of both half-spaces;
(2) displacements are functions only of the normal components (f) of the surface forces;
(3) forces are related to displacements through influence functions.

Considering a reference plane where $z = 0$, let w be the relative displacement between two points far from the interface, assumed as positive in the closure direction. The function $\Delta h(x, y)$ can be introduced, representing the *sum* of the heights of two corresponding points in the undeformed condition. The graph of this function represents a virtual invasive fractal surface (composite topography, or *delta-surface*, see Figure 3c) whose fractal dimen-

sion increases as the relative offset v increases, passing from 2.0 (corresponding to a flat plane obtained from the initially matching faces) to a value larger than 2.0 when correlations between the facing surfaces vanish. The following linear system of equations can be written

$$\frac{-w + \Delta h_r}{2} = \sum_s H_{rs} f_s, \qquad \forall P_r \in \mathcal{D}, \tag{3}$$

where f_s is the resultant of the forces acting on the contact spot around point P_s and $\mathcal{D}$ is the set of the points undergoing true contact. The influence terms H_{rs} can be evaluated by referring to the settlements induced by a unit load, applied to an elastic half space through a rigid plate acting at point P_s.

Solving the system of (3) by using a Gauss-Seidel iterative method, the contact forces between the two bodies are calculated, provided the contact domain $\mathcal{D}$ is first determined ($\mathcal{D}$ is not known *a priori*). The solution of this problem can be conveniently achieved by means of an incremental-iterative algorithm (*active set strategy*). For any given closure displacement w_i, an iterative procedure is started from a tentative domain $\mathcal{D}_i^{(1)}$ through a sequence of sets: $\mathcal{D}_i^{(k+1)} \subseteq \mathcal{D}_i^{(k)}$, $k = 1, \ldots, m-1$. At each step k, the system (3) is solved, retaining in the contact domain $\mathcal{D}_i^{(k+1)}$ only the points where compressive forces have been found (*unilateral contact condition*). The procedure converges to the correct domain $\mathcal{D}_i^{(m)}$ in a few steps, through successive elimination of tension points. Once the correct solution is reached for the given increment i, the closure w_{i+1} is imposed, passing to a new increment.

The aforementioned procedure is carried out, for any given surface, with different values of the resolution s. At each scale, a classical euclidean problem is solved, and in the limit of the finest resolution a fractal behaviour is achieved, as will be explained in the following.

With reference to Figure 3, the simulation has been carried out by considering a $20 \times 20\,\text{mm}^2$ central portion of crack surface, initially perfectly matching the opposite side. The portion can slide over the facing surface along two orthogonal directions in the $X - Y$ plane. The minimum relative offset v is equal to one pixel, (i.e., to $100\,\mu$m for the rock and to $80\,\mu$m for the concrete interface). The crack closure behaviour $(F - w)$, for each relative horizontal position, can be obtained by applying an increasing closure displacement and computing the corresponding total normal force. By varying v under constant normal force F, the crack opening δ can be computed, obtaining the crack dilatancy curves $(v - \delta)$. In all cases, the simulations provide the true contact domain at each step, plus the forces and displacements at any contact point.

5. Mechanical response

The problem of joint closure under normal loads is of great importance in rock mechanics, and can be relevant also for concrete dams and reservoirs. In Figure 4a, the closure curves obtained, for the rock interface, in correspondence of five different values of the relative shear displacement v (West direction in Figure 3a), are shown. The effective interface closure w_{int} can be estimated by subtracting, from the total displacement w, the part due to the elasticity of the half-spaces ($w_{\text{int}} = w - w_b$). The bulk contribution w_b depends only on F and can be evaluated by considering uniform pressure on the nominal loaded area. By fitting the data with a hyperbolic function, the asymptotes of the curves can be estimated, which correspond to the complete closure of the joints. It can be noticed that, as the initial offset v increases,

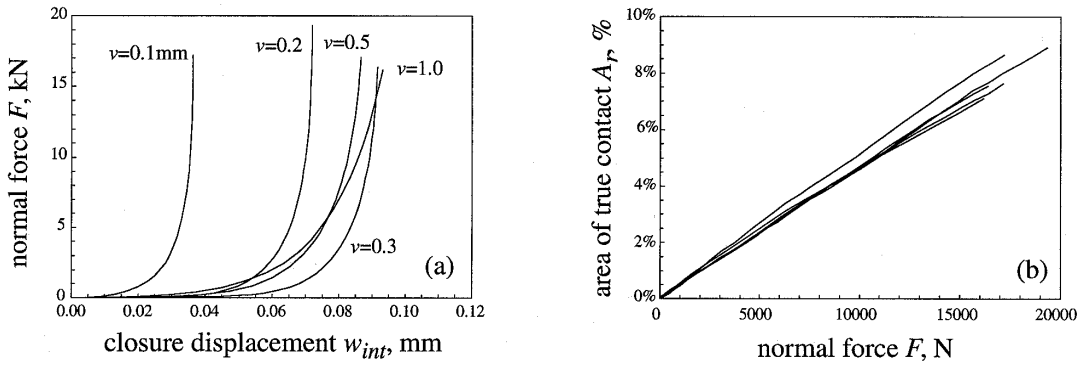

Figure 4. Crack closure laws (a) and plot of the real contact area vs. the applied force (b) for the rock interface (at fixed resolution).

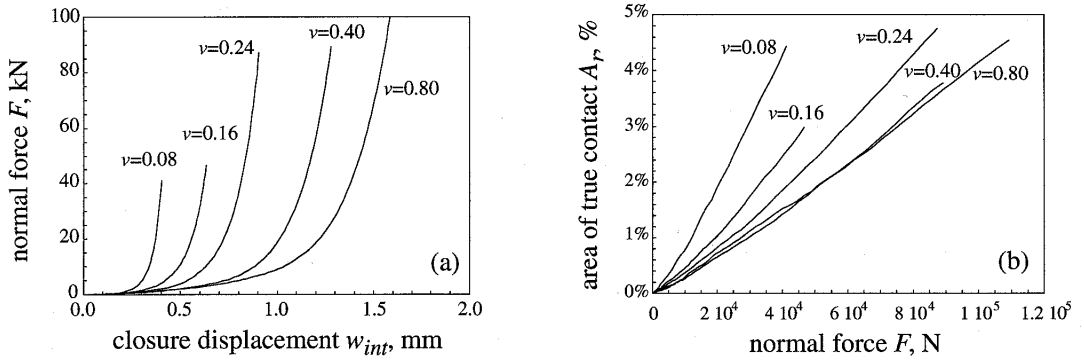

Figure 5. Crack closure laws (a) and plot of the real contact area vs. the applied force (b) for the concrete interface (at fixed resolution).

the extension of the closing stage increases, together with the interface compliance. This corresponds to the increase of the fractal dimension of the *delta-surface*, according to the results obtained with computer-generated surfaces by Borri-Brunetto et al. (1998). However, this is true only for the very initial stages of sliding. After a certain shear displacement ν, the curves overlap and the joint deformability becomes constant. On the other hand, when ν becomes very large ($\nu \approx 10$ mm), the joint compliance increases again because no more correlations are present between the opposite pushing surfaces (see the last contact domain in Figure 6).

The crack closure curves for the concrete interface are shown in Figure 5a. The same observations put forward for the rock interface apply also here. Independently of the relative shear displacement, the closure behaviour of natural joints undergoes size-effects, i.e, the larger the samples, the larger the closure deformability. In a previous paper by Borri-Brunetto et al. (1998), in fact, the authors compared the numerical load-displacement diagrams obtained for the larger surfaces with the diagrams obtained for the smaller surfaces and concluded that the joint closure deformability is larger for larger specimens, in agreement with the experimental data reported by Sage et al. (1990).

If the area of true contact is plotted versus the applied load, a nearly linear behaviour ($A_r \sim F$) is observed, both for the rock (Figure 4b) and for the concrete (Figure 5b) interfaces. This is in agreement with early theoretical arguments and with many experimental results

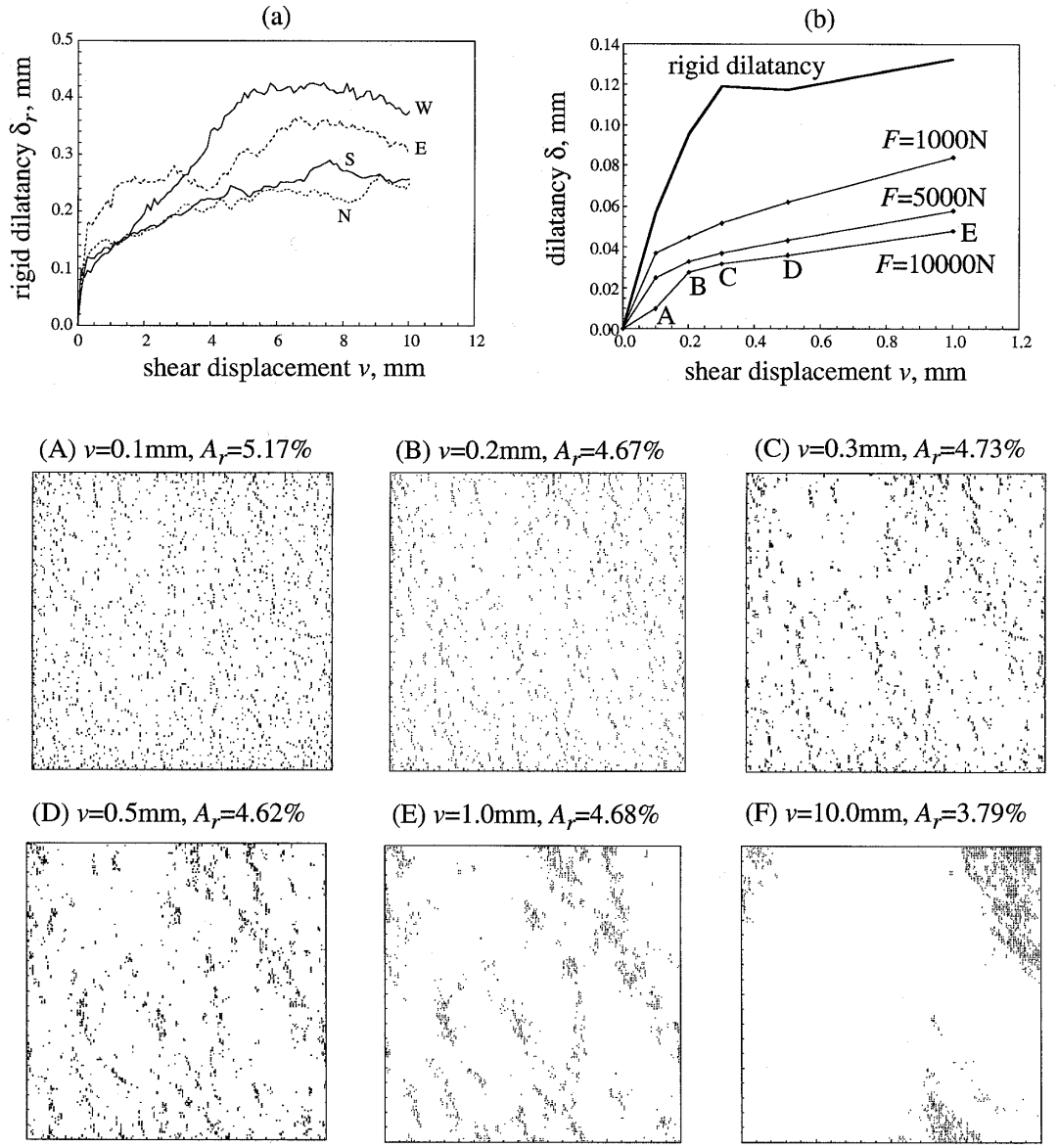

Figure 6. Rigid dilatancy curves (a), elastic curves (West direction) (b), and calculated contact domains corresponding to points $A - E$ on the $F = 10{,}000$N curve (rock interface).

(Johnson, 1985). However, as will be shown in the next section, because the euclidean measure of A_r depends on the measurement precision, the classical contact theories do not provide predictive capabilities. Suffices to notice, for now, the decrease of the area of true contact for a fixed value of F as the offset v increases. Significantly, this is especially evident in the case of concrete (Figure 5b).

The rigid-body dilatancy curves (corresponding to $F = 0$) of the rock interface are shown in Figure 6a for the four orthogonal directions. The curves have been obtained after detrending the mean crack plane. In this way, a horizontal plateau is reached. The elastic dilatancy δ, at

a fixed value of F, is computed by subtracting, from the rigid dilatancy δ_r, the joint closure displacement w_{int}

$$\delta(F, v) = \delta_r(v) - w_{\text{int}}(F, v) = \delta_r(v) - [w(F, v) - w_b(F)]. \tag{4}$$

The initial parts ($v \leqslant 1.0$ mm) of the elastic dilatancy curves obtained, in the West direction, for three values of F (1000N, 5000N and 10,000N, corresponding, respectively, to the nominal pressures of 2.5MPa, 12.5MPa and 25MPa), are shown in Figure 6b. The analysis of the dilatancy curves could allow for an estimation of the shear strength developed during sliding of rock rough interfaces. In fact, as commonly assumed, the effective value of the friction angle can be calculated as the sum of a basic angle and the current dilatancy angle (e.g. Goodman, 1989).

Six contact domains, generated in the rock interface for fixed $F = 10{,}000$N, are depicted in Figure 6. As already observed in Figure 4b, the larger the displacement v between the crack faces, the smaller the percentage of contact area, even if this trend is less evident than in the case of concrete. However, as v increases, the domains become less homogeneous and the contact points, initially spread almost uniformly, tend to cluster only in some zones. The last domain (F), corresponding to the *delta-surface* in Figure 3c, is different from the others, due to the relatively large offset (10 mm). No more correlations between the crack sides are present, suggesting the existence of a threshold scale, related to a characteristic length of the fracture surface or to an internal length of the material.

In the case of the concrete interface, the rigid-body dilatancy curves (corresponding to $F = 0$) are shown in Figure 7a, while three elastic curves are shown in Figure 7b. A marked anisotropy is revealed in this case. For the West and North sliding directions, the rigid dilatancy δ_r immediately raises to a plateau value $\delta_r \approx 2$ mm (corresponding to $v \approx 0.8$ mm), and then remains approximately constant under shear displacement. Instead, in the East and South directions, after a steep increasing stage, δ_r continues to grow, attaining an oblique asymptote. Six contact domains for $F = 30{,}000$N are shown in the same figure. Again, the larger the shear displacement v between crack faces, the smaller the percentage of true contact area. This is true up to a certain shear displacement, after which A_r seems to remain approximately constant (see also Figure 5b, comparing the curves for $v = 0.40$ mm and $v = 0.80$ mm). Note also that the last domain (F) is totally different from the others, due to the large shear displacement (8 mm). Localization of the contact spots is even more pronounced than in the case of the rock interface, probably due to macro-heterogeneities.

6. Fractal lacunarity of the contact domain and related size effects

The results presented up to now have been obtained for a fixed value of the discretization s. Such an approach is particularly important because any real measurement is always performed at finite resolution. However, to consider the scale-dependence of the model response, a multiresolution analysis has been performed. When the normal contact simulation is carried out, at a given offset, for a composite topography with given fractal dimension $\Delta_{\mathcal{G}}$ but with *different discretizations* s, the resulting contact domains $\mathcal{D}_s$ can be compared (Figure 8). A visual comparison with the experimental domain shown in Figure 1a (where the black *islands* are contact points, floating in an *ocean* where contact does not occur) confirms the consistency of the numerical simulations and suggests a deeper insight into the geometric structure of the contact domain.

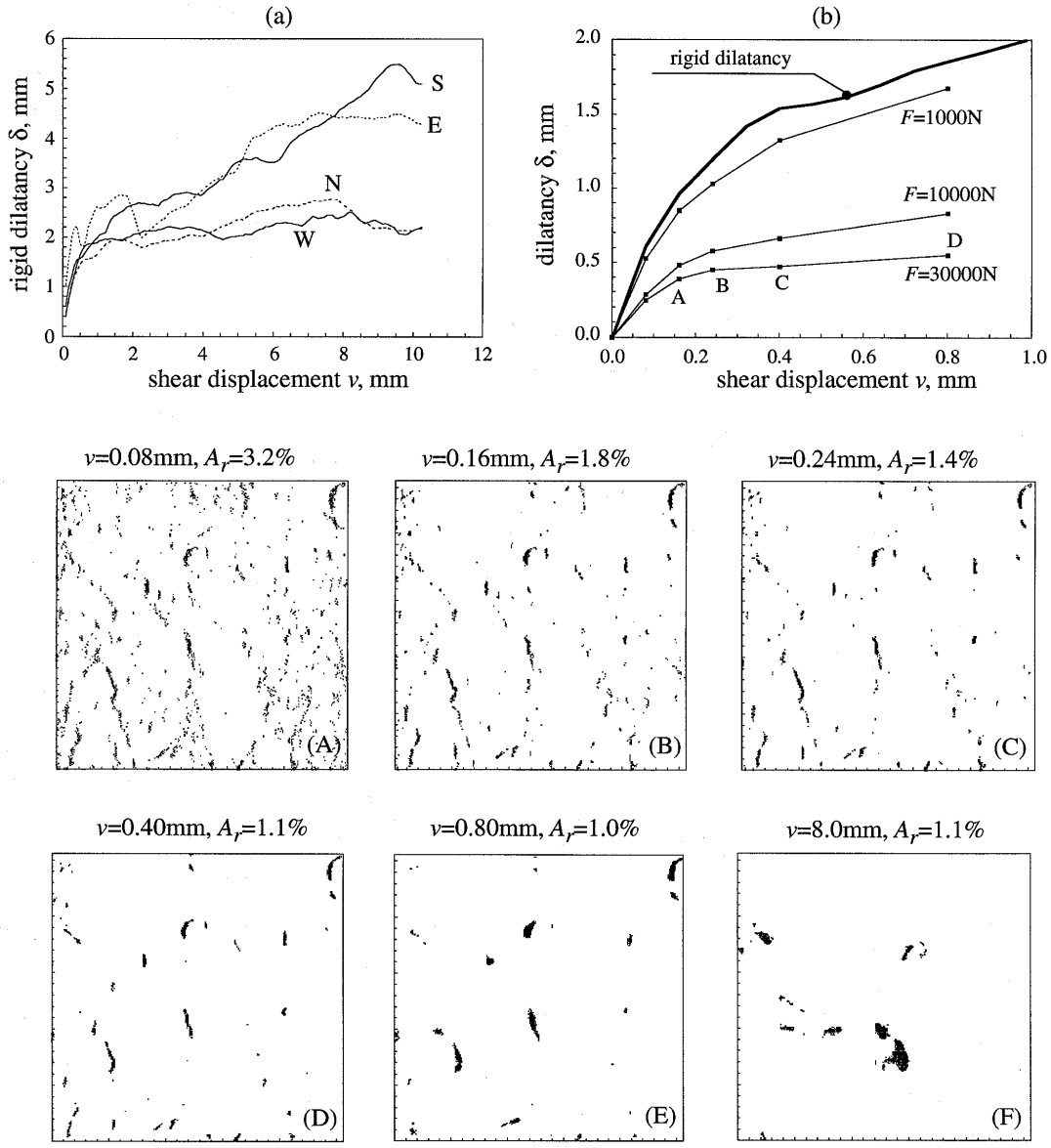

Figure 7. Rigid dilatancy curves (a), elastic curves (West direction) (b), and calculated contact domains corresponding to points $A - E$ on the $F = 30{,}000$N curve (concrete interface).

It can be easily realized that the concept of area of true contact, although representing a step forward with respect to the concept of apparent (nominally flat) area, is not able to describe consistently (that is, in a scale-independent manner) the interface interactions. As it clearly emerges from Figure 8 (which is relative to a mathematical joint), the real contact area A_r, at a fixed value of the normal pressure, progressively decreases with increasing the resolution of the discretization, ideally tending to zero in the theoretical limit of $s \to 0$. This power-law behaviour proves that the contact domain $\mathcal{D}$ is a *lacunar* (rarefying) fractal set in the plane, that is, a fractal set with null Lebesgue measure. This implies the necessity of abandoning

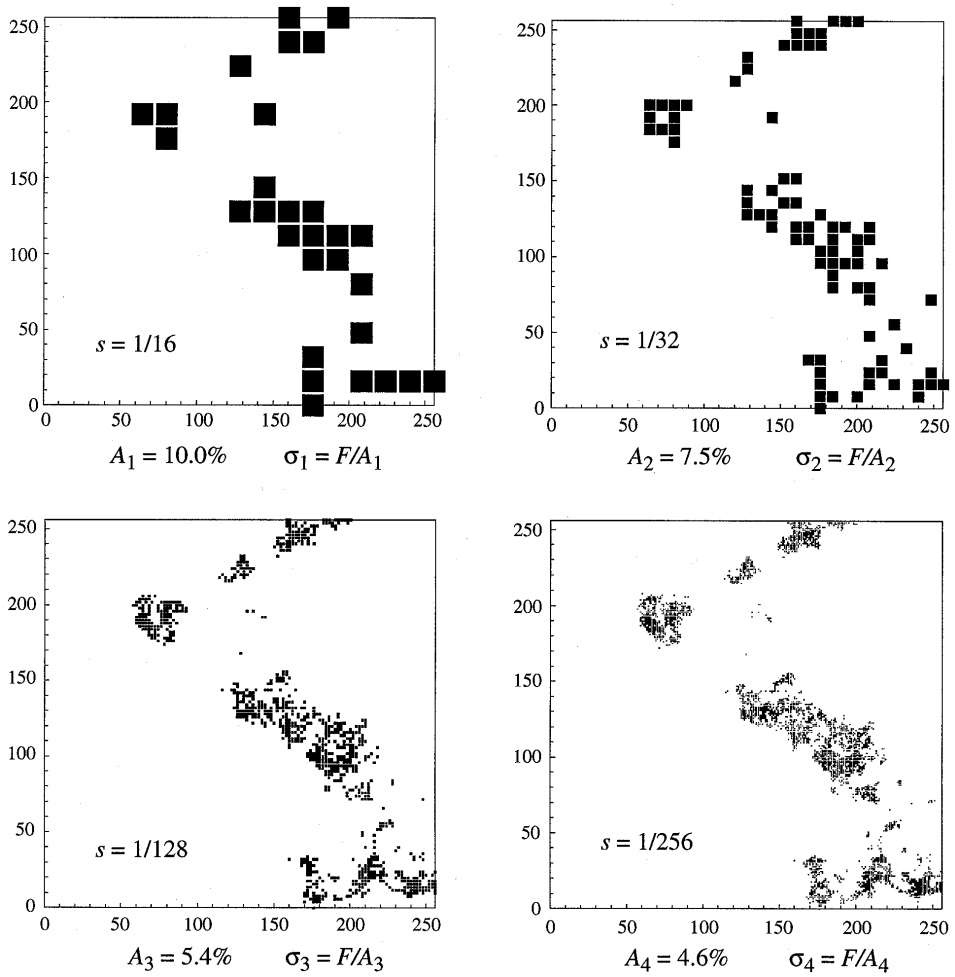

Figure 8. Decrease of the real contact area and increase of the corresponding real mean pressure (at fixed load) with increasing resolution (surface dimension $\Delta_{\mathcal{G}} = 2.1$, contact domain dimension $\Delta_\sigma = 1.39$).

the euclidean description and moving to the fractal model, characterized by the noninteger dimension $\Delta_\sigma (\Delta_\sigma \leqslant 2.0)$ of the domain $\mathcal{D}$.

Application of the *box-counting method* (Mandelbrot, 1982) to a large number of contact sets, obtained for different normal loads and various horizontal offsets, makes it possible to compute their fractal dimension Δ_σ (Figure 9). Note that the contact domains are, to a great extent, self-similar, that is, they show isotropic scaling. This is because they are related (but not coincident) to the so called *zero-sets* of the self-affine surfaces in contact, i.e., to the intersections of the surfaces with planes of equation $z = constant$ (Mandelbrot, 1985).

In perfect analogy with the theory of fractal scaling applied to nominal tensile strength (Carpinteri, 1994), let us consider the following renormalization group

$$F = \sigma_0 A_0 = \sigma_1 A_1 = \sigma_2 A_2 = \cdots = \sigma_n A_n = \cdots = \sigma^* \mathcal{H}_{\mathcal{D}}, \tag{5}$$

where F is the applied normal load (scale-invariant quantity), A_n and σ_n are respectively the real contact area ($[\mathrm{L}]^2$) and the real mean pressure ($[\mathrm{F}][\mathrm{L}]^{-2}$) measured at the pre-fractal

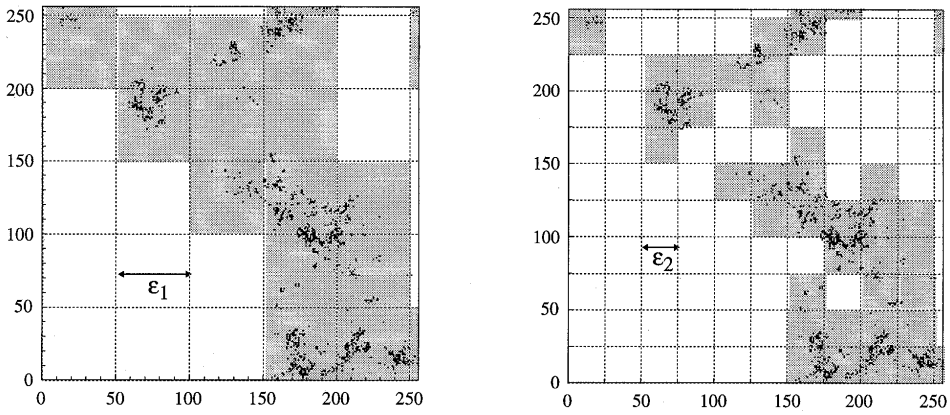

Figure 9. Box-counting method applied to the contact domain generated by a Brownian surface ($\Delta_{\mathcal{G}} = 2.5$) pushing against a flat plane.

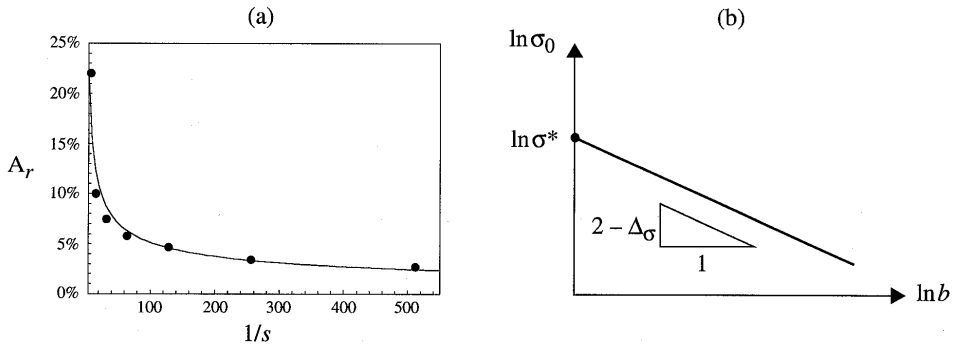

Figure 10. Computed power-law decrease of the real contact area with increasing resolution (a), and related scaling law for the nominal pressure (b).

resolution n, A_0 is the apparent (nominally flat) area and σ_0 is the apparent pressure. As one can realize from Figure 8, at any value of the normal load F, σ_n increases with increasing resolution and tends to infinity as $s \to 0$, because the euclidean measure ($[L]^2$) of the contact domain $\mathcal{D}$ vanishes (see Figure 10a, relative to a mathematical joint). Hence, in the limit of the highest resolution ($s \to 0$), the euclidean description loses its significance and leaves place to the *fractal measure* $\mathcal{H}_{\mathcal{D}}$ of the domain $\mathcal{D}$ (which is univocally defined only by the noninteger dimensionality $[L]^{\Delta_\sigma}$). Correspondingly, the *fractal mean pressure* σ^* can be defined as the anomalous flux of stress across the fractal interface. Owing to the dimensional homogeneity, this quantity holds the anomalous physical dimensions $[F][L]^{-\Delta_\sigma}$. By equating the second and the last term in (5) and taking the logarithm of both sides, if b is a characteristic linear size of the interface, the following scaling law is provided

$$\log \sigma_0 = \log \sigma^* - (2 - \Delta_\sigma) \log b. \tag{6}$$

In this context, if σ^* represents a scale-independent parameter governing the force flux across an interface, Equation (6) gives the dependence on the size of the specimen of the apparent normal pressure σ_0 required to activate that flux (Figure 10b). In other words, (6) allows to compute the size-dependent force F necessary to produce σ^* (and thus, possibly, to

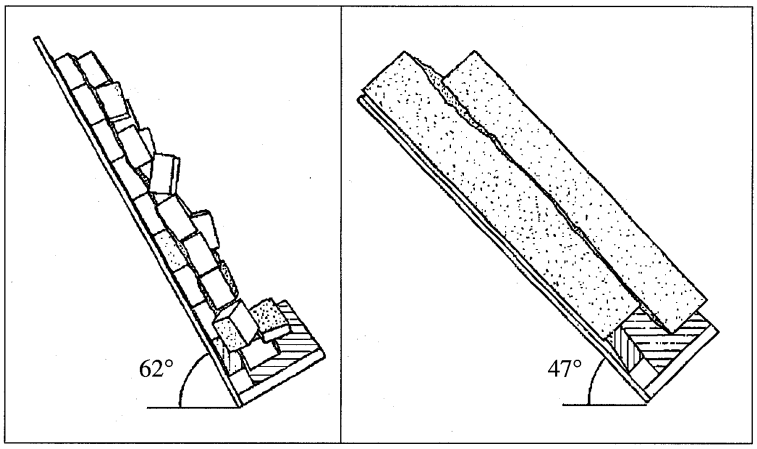

Figure 11. Experimentally detected size-scale effects on the limit slope angle (tilt tests after Bandis et al., 1981).

activate a certain friction) at the interface. In the case of euclidean interfaces, σ_0 would be the trivial governing parameter, and the classical $F \sim b^2$ scaling would be provided.

In close agreement with many experimental observations (Pinto da Cunha, 1993; Bandis et al., 1981), and assuming direct proportionality between the *fractal shear strength* τ^* and the fractal mean pressure $\sigma^*(\tau^* = \mu\sigma^*)$, Equation (6) affirms also that the apparent shear strength $\tau_0 = T/A_0$ decreases with increasing the size b of the nominal contact area (see also Figure 1b). This conjecture implies that the friction coefficient μ is not constant for a given interface but varies with its size. Thus, the limit slope angle decreases with increasing the specimen size (Figure 11). This approach may shed light on many rock slope instabilities, which are not explicable when compared to the relatively high friction values measured on smaller specimens.

Another fundamental aspect to be highlighted is the dimensional evolution of the contact domain $\mathcal{D}$, which is initially very rarefied (like a Cantor dust) and progressively increases its topological density with increasing the applied load (Figure 12). As the apparent pressure σ_0 increases, the classical theories yield the increase of the real contact area A_r (see the force vs. area laws in Figures 4b and 5b). Some relations can be found in the literature (Majumdar and Bhushan, 1990), connecting the area of true contact A_r and the real mean pressure $\sigma_r = F/A_r$ to the apparent pressure σ_0. However, since the euclidean measure of A_r depends on the measurement precision, the classical theories do not have unique predictive capabilities.

More significantly, the continuous variation of the box-counting dimension Δ_σ has to be considered. As the normal load F increases, Δ_σ starts from the value 0.0 (pointwise non-structured contact), then takes values comprised between 0.0 and 1.0 (pointwise contact sets which are structured, or self-similar, in a well-defined scale range), and subsequently takes values larger than unity as soon as linear contact structures and rarefied contact *islands* are formed. The total saturation of the contact domain $\mathcal{D}$ (or, at least, of some *islands*) would imply $\Delta_\sigma = 2.0$. It may be argued that this value, in real materials, could be attained only under very high normal loads, and this would imply an extended plastic deformation of the material, which is not contemplated in the numerical model.

According to the topological evolution of $\mathcal{D}$, the slope of the scaling law progressively decreases with increasing normal pressure (Figure 13). Note that also the fractal governing parameter σ^* is dependent on F, and therefore neither the slope, nor the intercept of the

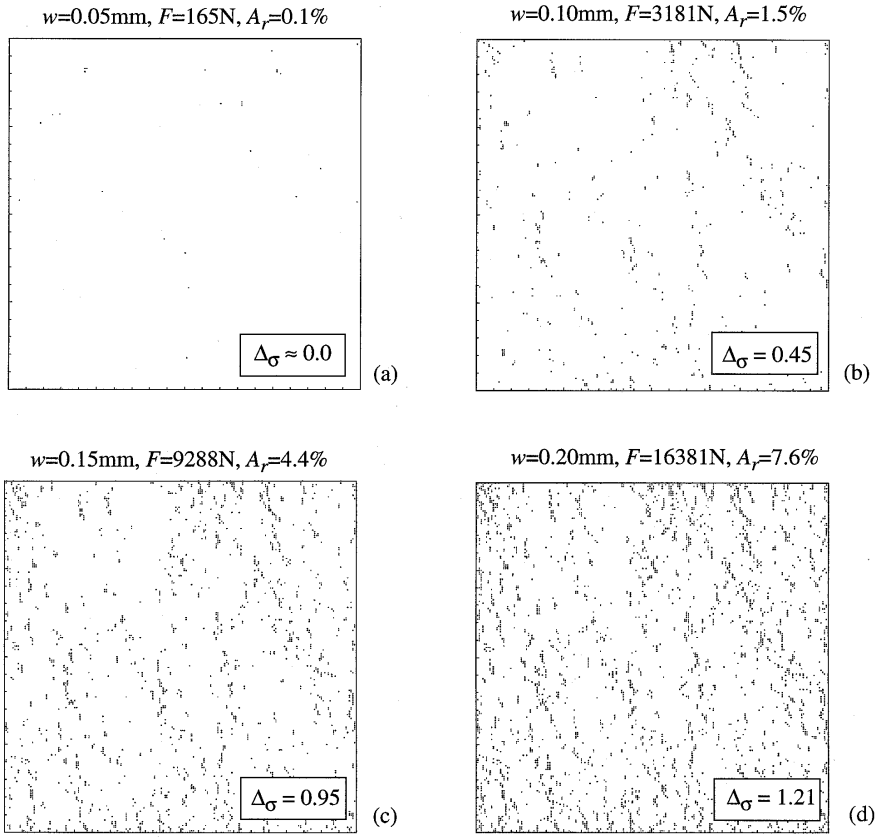

Figure 12. Evolution of the contact domain during closure of the rock joint (fixed offset $v = 0.3$ mm).

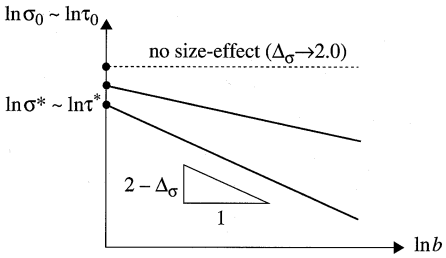

Figure 13. Size-scale effects on the nominal pressure (and on the nominal shear strength) for different lacunarities Δ_σ corresponding to different fractal mean pressures σ^*.

scaling law are unique, but vary with the load. In the limit case of $\Delta_\sigma = 2.0$, the euclidean description would be consistent. The physical quantities would retain their usual integer dimensions ($\sigma^* \to \sigma_0$) and a canonical scale-independent friction coefficient could be defined. Note that also in the model by Greenwood and Williamson (1966), the smooth behaviour is attained for very high loads.

7. Conclusions

In this paper, a numerical model has been presented for simulating the problem of normal contact between two elastic bodies with rough (fractal) boundaries. The model, although simple, captures some fundamental features of the mechanical problem, which can be easily extended to a wide class of interface phenomena, such as thermal and electric conductivity. The results of the simulations for a rock and a concrete interface are described, and the influence of fractality on the mechanical behaviour is discussed. The following conclusions may be traced.

- The higher the fractal dimension $\Delta_{\mathcal{G}}$ of the composite topography (related to the offset between the two facing sides of the crack), the higher the global closure deformability of the joint.
- Although the concept of area of true contact is ambiguous, the simulations, carried out at a pre-fractal level, yield a linear response in the normal load versus real area of contact diagram ($A_r \sim F$). Thus, the local self-affine complexity of the surfaces provides macroscopic linearity.

A completely new approach to the geometric structure of the contact domain (the horizontal projection of the set of points where contact truly occurs) has been put forward in the paper. A topologic analysis has shown that the real contact domain $\mathcal{D}$ is a *lacunar* fractal set in the two-dimensional plane, whose fractal (box-counting) dimension $\Delta_\sigma (\Delta_\sigma < 2.0)$ is progressively increasing with the load. As a major consequence, the physical quantities (mechanical stress, electricity or heat conductance) defined over this fractal set assume noninteger (anomalous) dimensions.

- The lacunarity of the contact domain $\mathcal{D}$ is proven numerically by the power-law scale-dependence of the real contact area A_r and of the real mean pressure $\sigma_r = F/A_r$.
- Assuming direct proportionality between shear strength and normal pressure, the decrease of the apparent shear strength $\tau_0 = T/A_0$ with increasing the size of the nominal contact area A_0 is obtained (size-scale effect). Hence, the friction coefficient μ is not constant for a given interface, but varies with its size.
- However, this size-dependence, which is more pronounced for larger fractal dimensions $\Delta_{\mathcal{G}}$ of the composite topography, progressively decreases as the nominal pressure increases.
- For a fixed value of Δ_σ, lacunarity implies that the contact domains of larger joints are less dense in the euclidean sense. This means that the probability of presence of large zones where contact does not occur increases with the size of the interface. This represents another way to justify the size effects on shear strength.

These preliminary conclusions suggest the possibility of re-interpreting the phenomenological friction laws on the basis of a fractal approach. However, further theoretical and experimental investigations are required to validate a scale-independent friction criterion based on a fractal mesomechanical framework.

Acknowledgements

Support by the Italian Ministry of University and Scientific Research and by the EC-TMR Contract N. ERBFMRXCT 960062 is gratefully acknowledged.

References

Archard, J.F. (1957). Elastic deformation and the laws of friction. *Proceedings of the Royal Society of London A* **243**, 190–205.

Bandis, S., Lumsden, A.C. and Barton, N.R. (1981). Experimental studies of scale effects on the shear behaviour of rock joints. *International Journal of Rock Mechanics, Mining Sciences and Geomechanics Abstracts* **18**, 1–21.

Barton, N. and Choubey, V. (1977). The shear strength of rock joints in theory and practice. *Rock Mechanics* **10**, 1–54.

Brown, S.R. and Scholz, C.H. (1985). Broad bandwidth study of the topography of natural rock surfaces. *Journal of Geophysical Research* **90**, 12575–12582.

Borodich, F.M. and Mosolov, A.B. (1992). Fractal roughness in contact problems. *Journal of Applied Mathemathics and Mechanics* **56**, 681–690.

Borri-Brunetto, M., Carpinteri, A. and Chiaia, B. (1998). Lacunarity of the contact domain between elastic bodies with rough boundaries. *Probabilities and Materials. Tests, Models and Applications*, NATO ASI Series 3 (Applied Sciences), Vol. 46, Kluwer Academic Publishers, Dordrecht, 45–64.

Carpinteri, A. (1994). Fractal nature of material microstructure and size effects on apparent mechanical properties. *Mechanics of Materials* **18**, 89–101.

Carpinteri, A., Chiaia, B. and Invernizzi, S. (1999). Three-dimensional fractal analysis of concrete fracture at the meso-level. *Theoretical and Applied Fracture Mechanics*, in print.

Cook, N.G.W. (1992). Natural joints in rock: mechanical, hydraulic and seismic behaviour and properties under normal stress. *International Journal of Rock Mechanics, Mining Sciences and Geomechanics Abstracts* **29**, 198–223.

Goodman, R.E. (1989). *Introduction to Rock Mechanics*, John Wiley & Sons, New York.

Greenwood, J.A. and Williamson, J.B.P. (1966). The contact of nominally flat surfaces. *Proceedings of the Royal Society of London A* **295**, 300–319.

Johnson, K.L. (1985). *Contact Mechanics*, Cambridge University Press, Cambridge.

Ling, F.F. (1989). The possible role of fractal geometry in tribology. *Tribology Transactions* **32**, 497–505.

Majumdar, A. and Bhushan, B. (1990). Role of fractal geometry in roughness characterization and contact mechanics of surfaces. *Journal of Tribology (ASME)* **112**, 205–216.

Majumdar, A. and Tien, C.L. (1990). Fractal characterization and simulation of rough surfaces. *Wear* **136**, 313–327.

Mandelbrot, B.B. (1982). *The Fractal Geometry of Nature*, W.H. Freemann & Company, New York.

Mandelbrot, B.B. (1985). Self-affine fractals and fractal dimension. *Physica Scripta* **32**, 257–260.

Panagiotopoulos, P.D. (1985). *Inequality Problems in Mechanics and Applications*, Birkhäuser Verlag, Basel.

Panagiotopoulos, P.D. and Panagouli, O.K. (1997). Fractal geometry in contact mechanics and numerical applications. *Fractals and Fractional Calculus in Continuum Mechanics* (Edited by A. Carpinteri and F. Mainardi), Springer-Verlag, Wien, 109–171.

Park, R. and Paulay, T. (1975). *Reinforced Concrete Structures*, Wiley, New York.

Pinto da Cunha, A. (Ed.) (1993). *Scale Effects in Rock Masses 93*, Balkema, Rotterdam.

Sage, J.D., Aziz, A.A. and Danek, E.R. (1990). Aspects of scale effects on rock closure. *Scale Effects in Rock Masses 90* (Edited by A. Pinto da Cunha), Balkema, Rotterdam, 175–181.

Schmittbuhl, J., Schmitt, F. and Scholz, C.H. (1995). Scaling invariance of crack surfaces. *Journal of Geophysical Research* **100**, 5953–5973.

Yoshinaka, R., Yoshida, J., Arai, H. and Arisaka, S. (1993). Scale effects on shear strength and deformability of rock joints. *Scale Effects in Rock Masses 93* (Edited by A. Pinto da Cunha), Balkema, Rotterdam, 143–149.

Yoshioka, N. and Scholz, C.H. (1989). Elastic properties of contacting surfaces under normal and shear loads. *Journal of Geophysical Research* **94**, 17681–17690.

Wang, W. and Scholz, C.H. (1993). Scaling of constitutive parameters of friction for fractal surfaces. *International Journal of Rock Mechanics, Mining Sciences and Geomechanics Abstracts* **30**, 1359–1365.

Warren, T.L. and Krajcinovic, D. (1995). Fractal models of elastic-perfectly plastic contact of rough surfaces based on the Cantor set. *International Journal of Solids and Structures* **19**, 2907–2922.